OZONE: SCIENCE & ENGINEERING
http://dx.doi.org/10.1080/01919512.2016.1188682

Taylor & Francis
Taylor & Francis Group

Optimization of Mixing and Mass Transfer in In-line Multi-Jet Ozone Contactors Using Computational Fluid Dynamics

Srikanth S. Pathapati, Angelo L. Mazzei, James R. Jackson, Paul K. Overbeck, Justin P. Bennett, and Cece M. Cobar

Mazzei Injector Company, LLC, Bakersfield, California, 93307, USA

ABSTRACT

Typical ozone mixing and mass transfer calculations are lumped approaches based on ideal operating conditions and can misrepresent behavior in real-life installations. This article models the effect of local hydrodynamics and mixing on the overall mass transfer of ozone into water with the aid of multiphase computational fluid dynamics (CFD). CFD models were validated with measured data from a pipeline ozone contactor installation which was optimized for more rapid, uniform mixing and mass transfer. Results emphasize the sensitivity of mixing quality to nozzle placement, size, orientation and spacing relative to main pipeline diameter and flows.

ARTICLE HISTORY
Received 29 March 2016
Accepted 9 May 2016

KEYWORDS
Ozone; Basin Nozzle Manifold; Computational Fluid Dynamics; Drinking Water Treatment; Fine Bubble Diffusion; Injection; Multi-Phase; Ozonation; Reactor Design; Retrofit; Side-Stream Venturi Injection

Introduction

Many ozone utility designs in recent years have opted for side-stream venturi injection (SVI) both for in-pipe contacting and for contact basins (Crittenden et al. 2012; Tchobanoglous et al. 2002; Rakness 2005). Transfer efficiency to the liquid phase is a crucial economic and operational consideration. For instance, unstable ozone residual readings can cause the supplying ozone generator to over-/underproduce ozone. SVI systems allow for a smaller footprint and stable ozone residual (Jackson, Meyer, and Bennett 2007; Mazzei, Meyer, and Bollyky 1995).

A typical ozone application is for odor control (Edwards-Brandt et al. 2007), specifically the removal of hydrogen sulfide from well water for odor control (Duranceau et al. 2010). Hydrogen sulfide (H_2S) is oxidized rapidly with ozone to form sulfate. The oxidation process proceeds in stages, first forming insoluble elemental sulfur. Further oxidation dissolves the elemental sulfur, forming soluble sulfite, and continued oxidation produces sulfate (Rakness 2005). More ozone is required to completely oxidize sulfide to sulfate than is required to produce the insoluble, colloidal elemental sulfur. In 2002, the Orlando Utilities Commission (OUC) installed an oxygen-fed (with supplemental nitrogen boost) ozone system utilizing diffuser contacting for the reduction of hydrogen sulfide at eight water treatment plants that are supplied water by sulfide-containing wells (Rakness 2005). OUC has since begun retrofitting these plants with oxygen-fed ozone generators, SVI and pipeline contactors for ozone contacting with the water.

Predicting the mass transfer and mixing performance of gas-liquid systems is fraught with complexity due to the possibility of remarkably distinct flow regimes such as slug flows, bubbly flows, annular and separated flows, often occurring within the same process. Each flow regime requires a targeted approach to resolve turbulence and phase interaction in order to quantify the degree of homogeneity of mixing. Inadequate mixing can result in less than desired exposure of ozone to the target. This may cause incomplete oxidation and subsequent formation of toxic and unwanted by-products.

Traditional modeling depends on broad assumptions and simplifications which may misrepresent actual flow conditions—this is especially crucial for multiphase flows in retrofit applications in the water/wastewater industry. Computational fluid dynamics (CFD) has been applied to environmental engineering in recent years, specifically in water and wastewater treatment (Do-Quang et al. 1998). CFD is a method to solve the Navier-Stokes equations for coupled fluid and gas dynamics using a series of discretization techniques and algorithms (Anderson and Wendt 1995; Versteeg and Malalasekera 1995).

CONTACT Srikanth S. Pathapati spathapati@mazzei.net Mazzei Injector Company, LLC, 500 Rooster Dr., Bakersfield, CA 93307, USA.
Color versions of one or more of the figures in the article can be found online at www.tandfonline.com/BOSE.

Generally, mass transfer equations assume completely mixed conditions and are based on equilibrium chemistry principles. Thus, there is a possibility of error in predictions using standard solubility curves and mass transfer coefficients under non-ideal flow conditions. In addition to achieving the required ozone mass transfer, a stable ozone residual and overall process control are crucial parameters that influence design. There may be situations where adequate mass transfer is achieved, but the ozone residual is unstable downstream. This leads to a situation where the measurement location will have to be deferred further away from the injection point, thus resulting in reduced CT credit. In addition, an unstable residual, when tied to an automated ozone dosing system, causes wide swings in the applied ozone dosage and generally results in higher ozone production costs. Rapid mixing and mass transfer are thus especially important for disinfection applications.

This article develops a CFD-based mass transfer model. This mass transfer model will focus on in-line multi-jet ozone contactors, also referred to as pipeline flash reactors in this article (PFR), combined with SVI. Mass transfer in PFRs occurs via three mechanisms. The first mechanism is the mixing of side-stream water with ozone at the injector. The second mechanism is the mixing of undissolved gas with the main flow, and the third mechanism is the mixing of ozone-saturated water with the main flow. This article reports studies of the effect on local mixing on the overall mass transfer of ozone into water in an in-line contacting system consisting of SVI and a PFR.

Methodology

Description of facility

The OUC Southwest WTP was designed to oxidize H_2S in 45.6 million gallons per day (MGD) well water with ozone produced by three 1,260 ppd oxygen-fed generators. The H_2S concentration range in the well water is 0.9–3.5 mg/L, depending on the well sources—at this specific plant the average concentration was measured to be 2 mg/L for design purposes. The temperature of the deep well water is nearly constant at 25.5 °C. The pH is approximately 7.5 units, hardness approximately 130 mg/L and alkalinity is approximately 110 mg/L. At this pH, 50% of total H_2S exists as un-ionized H_2S and the remaining 50% as HS^- ions. Mazzei designed a side-stream venturi injection system for odor control that utilized 5 venturi injectors, each feeding two nozzles. The system was designed to operate at flow rates ranging from a minimum daily flow of 10.4 MGD to a maximum flow of 45.6 MGD. Figure 1 and Figure 2 describe details of the installation. Immediately downstream of the pipeline flash reactor is a helical static mixer for additional mixing as well as an orifice mixing plate to provide additional mixing and backpressure. Treated water is routed to a contact basin downstream. The ozone residual is measured immediately prior to discharging into the contact basin.

CFD modeling methodology

Modeling methodology will be described in the following sequence—multiphase modeling, turbulence modeling, mass transfer modeling and species transport modeling.

Figure 1. Installation at OUC Southwest plant.

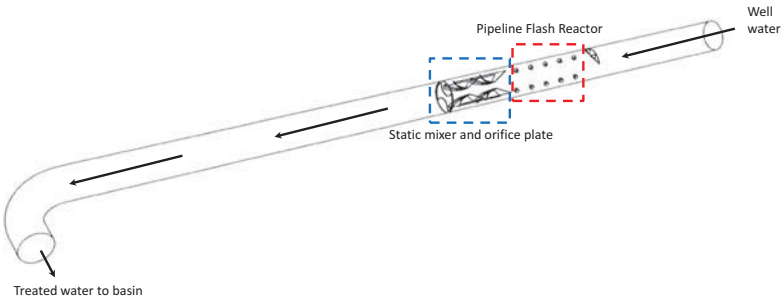

Figure 2. Process schematic.

Multiphase modeling

Typically, multiphase flows are modeled with a Eulerian–Eulerian approach or an Eulerian–Lagrangian approach (van Wachem et al. 2003). The latter is commonly accepted to be suited to modeling dilute flows, defined as flows with a second phase volume fraction (PVF) less than 10% (Brennen 2005). Because the gas volume fractions in this study exceed 10% (particularly at the nozzles and in their close vicinity), a Eulerian–Eulerian approach was utilized. Because the phase interaction is only in one direction—that is, the gas does not affect the behavior of the water, whereas the water affects the behavior of the gas—a simplified version of the Eulerian-Eulerian approach, namely the mixture model was utilized in this study.

The mixture model (Manninen, Taivassalo, and Kallio 1996) is used to model bubbly flows where phases move at different velocities. In the mixture model, phases are assumed to be interpenetrating. The mixture model solves the continuity equation for the mixture, the momentum equation for the mixture, the energy equation for the mixture, and the volume fraction equation for the secondary phases, as well as algebraic expressions for the relative velocities (if the phases are moving at different velocities).

The continuity equation for the mixture is written as follows:

$$\frac{\partial(\rho_m)}{\partial t} + div(\rho_m \bar{u}_m) = 0 \quad [1]$$

Where $\overline{u}_m$ is the mass-averaged velocity, defined as ρ_m is the mixture density, calculated as follows:

$$\rho_m = \sum_{k=1}^{n} \alpha_k \rho_k \quad [2]$$

Where α_k is the volume fraction of phase k.

The generalized momentum equation for the mixture can be obtained by summing the individual momentum equations for all phases. This is derived and solved for *x, y* and *z* components.

$$\begin{aligned}\frac{\partial}{\partial t}(\rho_m \vec{v}_m) + \nabla.(\rho_m \vec{v}_m \vec{v}_m) \\ = -\nabla p + \nabla.\left[\mu_m\left(\nabla \vec{v}_m + \nabla \vec{v}_m{}^J\right)\right] + \rho_m \vec{g} + \vec{F} \\ + \nabla.\left(\sum_{k=1}^{n} \alpha_k \rho_k \vec{v}_{dr,k} \vec{v}_{dr,k}\right)\end{aligned} \quad [3]$$

Where n is the number of phases, $\vec{F}$ is body force and μ_m is the viscosity of the mixture.

$\vec{v}_{dr,k}$ is the drift velocity for the secondary phase k calculated as:

$$\vec{v}_{dr,k} = \vec{v}_k - \vec{v}_m \quad [4]$$

The relative velocity (also referred to as the slip velocity) is defined as the velocity of a secondary phase (p) relative to the velocity of the primary phase (q).

$$\vec{v}_{pq} = \vec{v}_p - \vec{v}_q \quad [5]$$

The algebraic slip mixture model was utilized to model the slip velocity to account for the velocities of the gas and water phases.

Turbulent flow modeling

Hydrodynamics in the PFR vary as a function of *x, y* and *z* spatial coordinates. The dominant flow regime is turbulent in the PFR. A Reynolds averaged Navier–Stokes or RANS approach (Ferziger et al. 2002) was utilized to resolve turbulent flow. The RANS approach is based on "time averaging" the Navier–Stokes equations. This process yields additional terms in the standard transport equations, termed the "Reynolds stresses." In the standard k-ε model (Launder and Spalding 1974) for turbulent flow, a closed solution is obtained for the turbulent transport equations by relating Reynolds stresses to an eddy viscosity (μ_t). Newton's law of viscosity is applied to illustrate the relationship between viscous stresses and "Reynolds stresses." It should be noted that eddy viscosity (μ_t) is a nonphysical quantity, and is expressed by the following equation:

$$\mu_t = f\left(\frac{\rho k^2}{\varepsilon}\right) \quad [6]$$

In this expression, k is the turbulent kinetic energy per unit mass.

$$k = 0.5\left(\overline{u'^2} + \overline{v'^2} + \overline{w'^2}\right) \quad [7]$$

In this expression, u', v', w' are vector components of velocity fluctuations due to turbulence and ε is the dissipation rate of turbulent kinetic energy per unit mass. The transport equations of the standard k-ε model are expressed in the following equations:

For k:

$$\begin{aligned}\frac{\partial}{\partial t}(\rho k) + \frac{\partial}{\partial x_i}(\rho k u_i) = \frac{\partial}{\partial x_j}\left[\left(\mu + \frac{\mu_t}{\sigma_k}\right)\frac{\partial k}{\partial x_j}\right] + G_k \\ + G_b - \rho\varepsilon + S_k\end{aligned} \quad [8]$$

For ε:

$$\begin{aligned}\frac{\partial}{\partial t}(\rho\varepsilon) + \frac{\partial}{\partial x_i}(\rho\varepsilon u_i) = \frac{\partial}{\partial x_j}\left[\left(\mu + \frac{\mu_t}{\sigma_\varepsilon}\right)\frac{\partial \varepsilon}{\partial x_j}\right] \\ + C_{1\varepsilon}\frac{\varepsilon}{k}(G_k + C_{3\varepsilon}G_b) \\ - C_{2\varepsilon}\frac{\varepsilon^2}{k} + S_k\end{aligned} \quad [9]$$

In these expressions G_k represents generation of k due to the mean velocity gradients; G_b is generation of k due to buoyancy; $C_{1\varepsilon}$, $C_{2\varepsilon}$ and $C_{3\varepsilon}$ are experimental constants; σ_k and σ_ε are the turbulent Prandtl numbers for k and ε, respectively; S_k and S_ε are user-defined source terms. The constants were determined by Launder and Spalding (1974). It was hypothesized that isotropy of Reynolds stresses can be assumed reasonably in the case of the PFR. The values of $C_{1\varepsilon}$, $C_{2\varepsilon}$, $C_{3\varepsilon}$, σ_k and σ_ε used in the model are 1.44, 1.92, 0.09, 1.0 and 1.3, respectively (Launder and Spalding 1974). The no-slip boundary condition, along with effects of viscous blocking and kinematic damping creates large gradients in solution variables near the walls of the PFR. To account for these phenomena in the turbulence model, semi-empirical "wall functions" for the k-ε model were used.

Mass transfer modeling

Previous studies on ozone mass transfer modeling have focused on bubble columns, packed towers and baffled contactors (Cockx et al. 1999; Gong et al. 2007; Quiñones-Bolaños, Zhou, and Otten 2002; Wols et al. 2010; Zhang et al. 2007). In contrast to bubble diffusers, mass transfer and mixing in a pipeline flash reactor is more rapid and takes place in a highly turbulent environment. The following procedure was utilized to model mass transfer in this study.

Transfer of ozone in gas form to ozone in dissolved form was modeled by utilizing a subroutine that checked the concentration of ozone in each cell at the end of each numerical iteration. The concentration in each cell in the computational domain is a function of the volume of that cell that is occupied by dissolved versus gaseous ozone. That, in turn, is a function of the solved local velocity in three dimensions. If the concentration of ozone in the cell is equal to or greater than the saturation concentration of ozone per Henry's law, then ozone in the gas phase is allowed to dissolve in the water. This subroutine is based on the two-film model of gas-liquid mass transfer (Beltran 2003; Rakness 2005), where the flux, J is defined as:

$$J = k_L a\left(C_L^* - C_L\right) \quad [10]$$

Where k_L is the local liquid mass transfer coefficient, a is specific interfacial area, C_L* is the saturation concentration of dissolved ozone and C_L is the local concentration of ozone.

A large number of relationships exist for k_La calculation for bubble columns (Quiñones-Bolaños, Zhou, and Otten 2002). However, very few k_La studies have been performed for large scale in-line contactors. Applying k_La values from literature for bubble columns resulted in a significant deviation in predicted mass transfer efficiency. Subsequently, an iterative process was then utilized to calibrate the rate constant to match the mass transfer noticed at one measured test point. The initial estimate was based on a previous bench-scale study of mass transfer efficiency in pipeline flash reactors (Baawain et al. 2011). The k_La determined thus was then kept constant for three validation test points. It is noted that ozone decay is not modeled separately, as it will be included in the calibrated k_La.

Reactive species transport modeling

The following parameters were utilized in this study (mentioned previously and restated here) based on experimental measurements of water quality of sulfide-containing wells in Florida (Rakness 2005). The average H_2S concentration range is 2 mg/L. The temperature of the deep well water is nearly constant at 25.5 °C. The pH is approximately 7.5 units, hardness approximately 130 mg/L and alkalinity is approximately 110 mg/L. At this pH, 50% of total H_2S exists as un-ionized H_2S and the remaining 50% as HS^- ions.

The general stoichiometric relations that describe the reaction of ozone with H_2S are as follows:

$$H_2S + O_3 \rightarrow S + O_2 + H_2O \quad [11]$$

$$S^{2-} + 4O_3 + 4H_2O \rightarrow SO_4^{2-} + 4O_2 \quad [12]$$

Previous work (Mark, Naumov, and Von Sonntag 2011; Overbeck 1995) has suggested that the yield of SO_4^{2-} is 1 mol per 2.4–2.46 mol of ozone. However, accounting for ozone demand, OUC has typically used a dosage where the O_3/H_2S ratio is 4:1 (Rakness 2005). The actual average applied ozone dose at the OUC SW WTP was 9.1 mg/L, for the installation modeled in this study. At this dose of ozone, the hydrogen sulfide is almost instantaneously oxidized to sulfate. The generalized conservation equation for species transport is written as follows:

$$\frac{\partial}{\partial t}(\rho Y_i) + \nabla.(\rho \vec{v} Y_i) = -\nabla.\vec{J}_i + R_i + S_i \quad [13]$$

Where R_i is the net rate of production of species "i" by the defined chemical reaction. S_i is rate of creation by addition from the dispersed phase and from any other sources. A unidirectional Finite-Rate model was utilized to model the oxidation process of hydrogen sulfide by ozone. The inputs to the model included the rate constant. The rate constants were based on previous work by Mark, Naumov, and Von Sonntag (2011). However, as expected, rate constants derived under controlled conditions failed to predict the mass transfer of ozone with the desired accuracy. An iterative

process was then utilized to calibrate the rate constant to match the mass transfer noticed in one measured data point. This was then kept constant for all the other simulations.

Discretization and solution schemes

The computational geometry was discretized using an unstructured mesh with tetrahedral elements, shown in Figure 3. The TGrid (Qi and Lin 2006) algorithm was used to generate the mesh. A Finite Volume Method (FVM) was used to convert the governing equations to algebraic equations. A cell-centered scheme was used in the process of discretization. Values of cell faces were computed using a Second-Order Upwind Scheme (Barth and Jespersen 1989). The Second-Order Upwind Scheme is typically suggested as a requirement to procure accurate results with unstructured meshing schemes (ANSYS 2011).

Pressure-velocity coupling is an issue that must be addressed during the process of obtaining a sequential solution to the momentum and continuity equations. The SIMPLE (Semi-Implicit Method for Pressure Linked Equations) algorithm (Patankar 1980) was used to introduce a pressure term in the continuity equation. The SIMPLE algorithm was chosen as the consistent approach to pressure-velocity coupling across the range of operating flow rates. The criterion for iterative convergence was set at 1×10^{-9}, which is a typical constraint for multiphase flows that consider chemical kinetics (Ranade 2002).

Results

In order to quantitatively define the extent of mixing, a variable named "Uniformity Index" (UI) was utilized. UI represents how the gas phase varies over a defined surface, where a value of 1 indicates the highest uniformity. The area weighted UI captures the variation of the quantity (for example; the species concentration). The area-weighted UI of the gas phase was calculated using the following equation:

$$UI = 1 - \frac{\sum_{i=1}^{n} \left[\left(\left| \phi_i - \overline{\phi_a} \right| \right) A_i \right]}{2 \left| \phi_a \right| \sum_{i=1}^{n} A_i} \quad [14]$$

Where i is the facet index of a surface with facets, $\bar{\phi}_a$ is the average value of the gas phase volume fraction over the outlet boundary, given as follows:

$$\overline{\phi_a} = \frac{\sum_{i=1}^{n} \phi_i A_i}{\sum_{i=1}^{n} A_i} \quad [15]$$

Grid independence

As a first step towards ensuring numerical accuracy, grid independence was tested. Briefly, a solution is said to be grid-independent when progressively finer meshes do not affect model predictions. Figure 4 depicts the effect of finer meshes on predicted UI in the PFR. Grid independence is achieved at a mesh density of approximately 9.1 million computational cells.

Model validation

The model was validated by utilizing the calibrated $k_L a$ and reaction rate constant for three test points. The measured mass transfer efficiency (*MTE*) was compared to the modeled mass transfer efficiency. Relative percent difference (*RPD*) was chosen as a parameter by means of which to compare the measured data with the modeled data. *RPD* was calculated as follows:

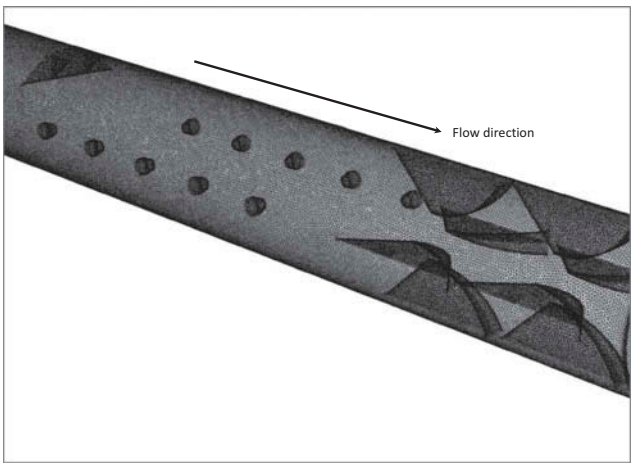

Figure 3. Computational mesh of the pipeline, test point 1.

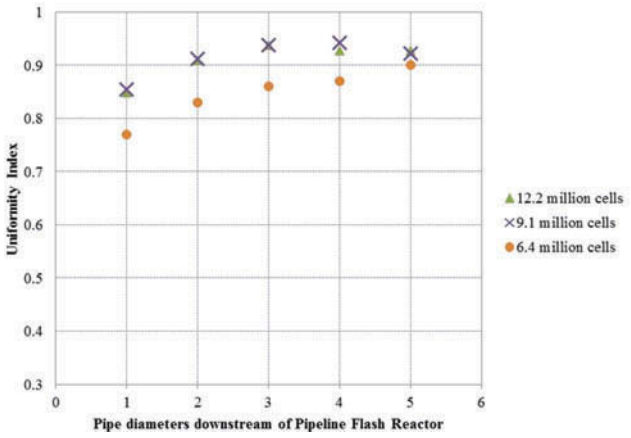

Figure 4. Grid independence.

$$RPD = 100 \times \left(\frac{Measured\ MTE - Modeled\ MTE}{Measured\ MTE}\right) \quad [16]$$

Results are presented in Table 1. Test point 1 is the calibration point for k_La and the reaction rate constant for H_2S and ozone. Test points 2, 3 and 4 are validation test points. All flow rates and ozone mass transfer data are from field measurements.

Results indicate that the model tends to underpredict MTE at higher flow rates. It is hypothesized that the higher turbulence and hence dissipation in the pipeline contactor at high flow rates could be the cause for this. Overall, the CFD model predicts MTE with an error less than 2%.

Figure 5 depicts contours of ozone concentration across a horizontal (top view) and a vertical (side view) plane, respectively, for test point 2. Visual inspection reveals that the ozone concentration is mostly uniform across the cross-section of the pipe, almost immediately after side-stream injection with optimized nozzles. It is also noticed that most of the transfer occurs rapidly, in the close vicinity of the jetting nozzles. This can be correlated to mixing uniformity. To obtain this optimal mixing, various configurations of nozzles were tested using CFD. Parameters that were analyzed included nozzle sizing, nozzle velocity, spacing between nozzles, nozzle orientation, nozzle penetration into the main pipeline, mainline velocity, side-stream ratio and gas to liquid ratio. Figure 6 depicts mixing UI as a function of each PFR configuration. Each value represents the average UI across a radial cross-section.

Conclusions

CFD combines computational methods with engineering physics, chemistry and mathematics to solve fluid flow challenges. A CFD approach to examining and modeling multiphase hydrodynamics provides an in-depth insight into flow patterns, mixing, mass transfer and chemical species transport, which in turn allows design engineers to make informed decisions and offer innovative solutions to lower cost and improve performance. Result of this study indicate that CFD can successfully be utilized to model mixing and mass transfer in SVI-based pipeline contactor systems. An advantage of pipeline contacting is that it removes the mixing uncertainty caused by phenomena such as short-circuiting seen in contact basin and the bulk of the water can be contacted in a controlled manner. In addition, rapid transfer combined with a uniform mix can allow for CT credit to be applied significantly earlier in the system.

It is important to note that optimal mixing combined with a carefully engineered corresponding ozone dose translates to rapid and uniform mass transfer. To

Table 1. Comparison of measured and modeled mass transfer efficiency.

Test point (TP)	Number of nozzles in use	Main flow rate (gpm)	Total side-stream water flow rate (gpm)	Total gas flow (side-stream) (scfm)	Mass transfer efficiency (%)		Relative percent difference (RPD) (%)
					Measured	Modeled	
TP 1 (calibration)	4	9583	1180	88	87.3	88.5	+1.4
TP 2 (validation)	4	9,583	1190	69	90.9	92.4	+1.6
TP 3 (validation)	4	13,264	1181	94	99.1	97.8	−1.3
TP 4 (validation)	6	20,972	2150	141	98.8	96.9	−1.9

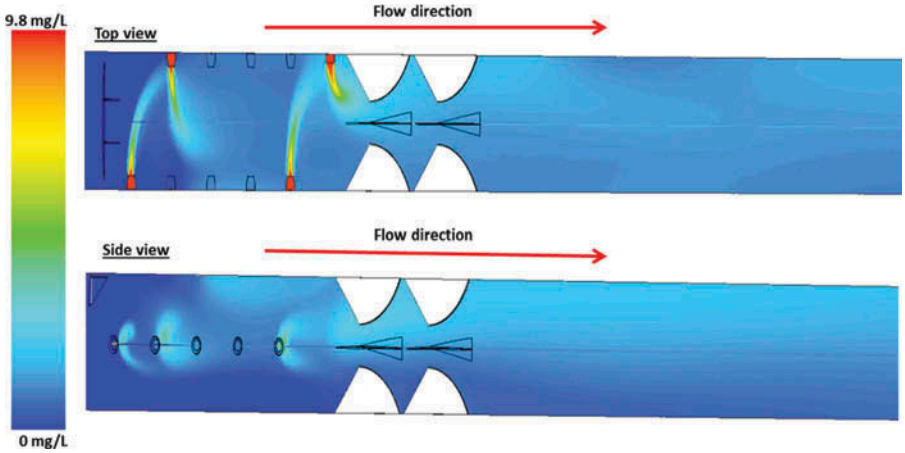

Figure 5. Contours of ozone concentration in the PFR, test point 1.

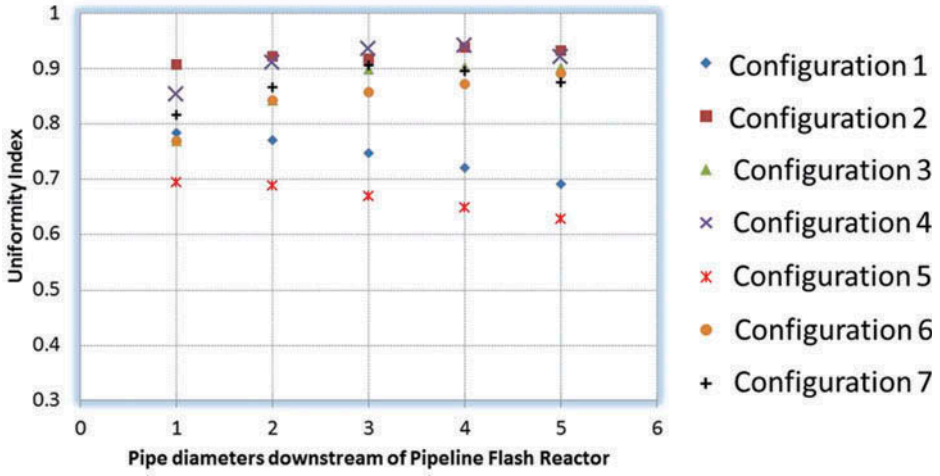

Figure 6. Mixing uniformity as a function of PFR configuration. Each configuration is a unique combination of nozzle velocity, spacing between nozzles, nozzle orientation, nozzle penetration into the main pipeline, mainline velocity, side-stream ratio and gas to liquid ratio.

optimize mixing, variables including but not limited to nozzle sizing, nozzle velocity, spacing between nozzles, nozzle orientation and nozzle penetration into the main pipeline should be investigated. This is especially crucial for retrofits where the ozonation system has to function within the constraints of existing upstream and downstream processes and plumbing. Further validation of the model is in process, as newer plant data becomes available.

References

Anderson, J. D., and J. F. Wendt. 1995. *Computational Fluid Dynamics*. New York, NY: McGraw-Hill.

ANSYS. 2011. *ANSYS Fluent14.0 Theory Guide*. Lebanon, NH: ANSYS Inc.

Baawain, M. S., M. Gamal El-Din, D. W. Smith, and A. Mazzei. 2011. "Hydrodynamic Characterization and Mass Transfer Analysis of an In-Line Multi-Jets Ozone Contactor." *Ozone: Science & Engineering* 33 (6):449–62. doi:10.1080/01919512.2011.622705.

Barth, T. J., and D. Jespersen 1989. "The Design and Application of Upwind Schemes on Unstructured Meshes." Technical Report AIAA-89-0366 presented at AIAA 27th Aerospace Sciences Meeting, Reno, Nevada, USA, January 9.

Beltran, F. J. 2003. *Ozone Reaction Kinetics for Water and Wastewater Systems*. Boca Raton, FL: CRC Press.

Brennen, C. 2005. *Fundamentals of Multiphase Flow*, 1st ed. New York, NY: Cambridge University Press.

Cockx, A., Z. Do-Quang, A. Line, and M. Roustan. 1999. "Use of Computational Fluid Dynamics for Simulating Hydrodynamics and Mass Transfer in Industrial Ozonation Towers." *Chemical Engineering Science* 54 (21):5085–90. doi:10.1016/S0009-2509(99)00239-0.

Crittenden, J. C., R. R. Trussell, D. W. Hand, K. J. Howe, and G. Tchobanoglous. 2012. *MWH's Water Treatment: Principles and Design*. Hoboken, NJ: John Wiley & Sons.

Do-Quang, Z., A. Cockx, A. Line, and M. Roustan. 1998. "Computational Fluid Dynamics Applied to Water and Wastewater Treatment Facility Modeling." *Environmental Engineering and Policy* 1 (3):137–47. doi:10.1007/s100220050015.

Duranceau, S. J., V. M. Trupiano, M. Lowenstine, S. Whidden, and J. Hopp. 2010. "Innovative Hydrogen Sulfide Treatment Methods: Moving beyond Packed Tower Aeration." *Florida Water Resources Journal*. July: 4–14

Edwards-Brandt, J., H. Shorney-Darby, J. Neemann, J. Hesby, and C. Tona. 2007. "Use of Ozone for Disinfection and Taste and Odor Control at Proposed Membrane Facility." *Ozone: Science & Engineering* 29 (4):281–6. doi:10.1080/01919510701459550.

Ferziger, J. H., and M. Peric. 2002. *Computational Methods for Fluid Dynamics*. Berlin, Germany: Springer Science & Business Media.

Gong, X., S. Takagi, H. Huang, and Y. Matsumoto. 2007. "A Numerical Study of Mass Transfer of Ozone Dissolution in Bubble Plumes with an Euler–Lagrange Method." *Chemical Engineering Science* 62 (4):1081–93. doi:10.1016/j.ces.2006.11.015.

Jackson, J. R., R. M. Meyer, and J. P. Bennett. 2007. "After a Decade of Development: A Profile of Municipal Drinking Water Plants Utilizing a Side-stream Injection Process." *Ozone: Science & Engineering* 29 (4):297–302. doi:10.1080/01919510701462679.

Launder, B. E., and D. B. Spalding. 1974. "The Numerical Computation of Turbulent Flows." *Computer Methods in Applied Mechanics and Engineering* 3:269–89. doi:10.1016/0045-7825(74)90029-2.

Manninen, M., V. Taivassalo, and S. Kallio. 1996. *On the Mixture Model for Multiphase Flow*. Technical Research Centre of Finland. Espoo, Finland: VTT Publications.

Mark, G., S. Naumov, and C. Von Sonntag. 2011. "The Reaction of Ozone with Bisulfide (HS–) in Aqueous Solution–Mechanistic Aspects." *Ozone: Science & Engineering* 33 (1):37–41. doi:10.1080/01919512.2011.536902.

Mazzei, A. L., R. M. Meyer, and L. J. Bollyky. 1995. "Mass Transfer of High Concentration Ozone with Efficiency Injectors and Degassing Separators." *International Ozone Association Pan American Group* 1:230–5.

Overbeck, P. K. 1995. "Ground Water Color and Sulfide Reduction with Ozone." *Proceedings of the Annual Conference of the American Water Works Association* published by American Water Works Association, Denver CO, 241–9.

Patankar, S. 1980. *Numerical Heat Transfer and Fluid Flow*, 1st ed. Washington, DC: Hemisphere Publishing Corporation.

Qi, D., and W. Lin 2006. "Tgrid: A New Grid Environment." Paper presented in International Multi-Symposiums on Computer and Computational Sciences, Zhejiang, PRC, June 20–24.

Quiñones-Bolaños, E., H. Zhou, and L. Otten 2002. "Computational Analysis of Ozonation in Bubble Columns." Paper presented in EWRI of ASCE Environmental Engineering Conference, Niagara Falls, Ontario, Canada.

Rakness, K. L. 2005. *Ozone in Drinking Water Treatment: Process Design, Operation, and Optimization*, 1st ed. Denver, CO: American Water Works Association.

Ranade, V. V. 2002. *Computational Flow Modeling for Chemical Reactor Engineering*, 1st ed. London, UK: Academic Press.

Tchobanoglous, G., F. L. Burton, and H. D. Stensel. 2002. *Wastewater Engineering: Treatment, Disposal, and Reuse*, 4th ed. New York, NY: McGraw Hill.

Van Wachem, B. G. M., and A. E. Almstedt. 2003. "Methods for Multiphase Computational Fluid Dynamics." *Chemical Engineering Journal* 96:81–98. doi:10.1016/j.cej.2003.08.025.

Versteeg, H., and W. Malalasekera. 1995. *An Introduction to Computational Fluid Dynamics: The Finite Volume Method Approach*, 1st ed. London, UK: Prentice Hall.

Wols, B. A., J. A. M. H. Hofman, W. S. J. Uijttewaal, L. C. Rietveld, and J. C. Van Dijk. 2010. "Evaluation of Different Disinfection Calculation Methods Using CFD." *Environmental Modeling and Software* 25:573–82. doi:10.1016/j.envsoft.2009.09.007.

Zhang, J., P. M. Huck, W. B. Anderson, and G. D. Stubley. 2007. "A Computational Fluid Dynamics Based Integrated Disinfection Design Approach for Improvement of Full-Scale Ozone Contactor Performance." *Ozone: Science and Engineering* 29 (6):451–60. doi:10.1080/01919510701613420.